

Time-resolved magnetization-induced second-harmonic generation from the Ni(110) surface

H. Regensburger, R. Vollmer, and J. Kirschner

Max-Planck-Institut für Mikrostrukturphysik, Weinberg 2, D-06120 Halle/Saale, Germany

(Received 5 November 1999)

Relaxation processes on the picosecond and subpicosecond time scale after optical excitation have been studied by time-resolved magnetization-induced second-harmonic generation from ferromagnetic nickel. A fast drop of the second-harmonic intensity and the Kerr-signal within 300 fs after optical excitation has been observed which is followed by a partial recovery within a few picoseconds. We show that the fast initial drop cannot be unambiguously attributed to an ultrafast decrease of the magnetization.

I. INTRODUCTION

The investigation of ultrafast magnetization dynamics has attracted much attention in recent years. The spin relaxation time, defined as the time elapsed until the direction of the spin is restored to the original direction after a (small) perturbation from the equilibrium direction, is of the order of about 100 ps to several ns as determined from the linewidth of spectroscopic measurements such as ferromagnetic resonance or Brillouin light scattering. Recently, this relaxation process has been observed directly in the time domain by several groups by measuring time-resolved magneto-optical Kerr effect (MOKE) (Refs. 1–3) or magnetization-induced second-harmonic generation (MSHG) (Ref. 4) after an ultrashort magnetic field pulse. Ju *et al.*³ measured the time dependence of MOKE from a ferromagnetic Ni layer on a NiO antiferromagnet after thermal depinning of the ferromagnetic layer by a preceding pump pulse in a reversed bias field. In all cases the time dependence of the Kerr signal could be well described by the usual Landau-Lifschitz equation with a characteristic oscillation frequency in good agreement with the spin wave frequencies known from spectroscopic measurements. The decay time of this oscillation is the spin-lattice relaxation time. Also the domain pattern of a Co/Pt film obtained after a strong transverse magnetic field pulse of ≈ 4 ps duration was in quantitative agreement with the above model.⁵

In 1991 Vaterlaus *et al.* found a rapid decay (within 100 ps) of the spin polarization of photoelectrons emitted from a gadolinium sample after a thermal excitation by a laser pulse.⁶ This decay time was also interpreted as the spin-lattice relaxation time. However, by using time-resolved MOKE in 1996 Beaurepaire *et al.* found a drop of the transient Kerr signal within the time resolution of the experiment of less than 2 ps.⁷ The signal partially recovered within a few ps. A similar behavior has been found since then by time-resolved MOKE (Refs. 8,9) and MSHG.^{10–12} A decay time of less than 30 fs was observed.¹¹ The almost instantaneous decay of the Kerr-signal was interpreted as an ultrafast demagnetization. Clearly, at such a short time scale this process cannot be caused by spin-lattice relaxation as those observations described in Refs. 1–4 cited in the first paragraph but must be of purely electronic origin. A theoretical model describing the time-dependent magneto-optical response on the fs time scale has been presented recently.^{13,14}

A similar effect has been observed in the two-photon photoemission from thin Ni films.¹⁵ The spin polarization of the photoelectrons dropped within 1 ps to a lower value. However, a second drop at much later times of about 500 ps was observed, which was not detected in the Kerr measurements mentioned above. The authors interpreted the first fast drop to be caused by the creation of Stoner excitation while the latter was assigned to the excitation of spin waves. Note the difference in interpretation to the Kerr measurements: As long as the excited electrons do not leave the crystal as in Ref. 15 spin-flip *e-e* scattering does not reduce the total spin polarization of the system and consequently the magnetization remains largely unaffected. (Only the weak probability of creation of Stoner excitations by the light during the pump pulse would reduce the magnetization.)

In this paper we focus on the time resolved MSHG measurements. We show that in the sub-ps time scale the magnetization induced part of the second-harmonic (SH) response is strongly affected by electronic changes induced by the preceding pump light pulse making it difficult to extract any information about the magnetization on this time scale. The remainder of the paper is organized as follows. After a short description of the experimental setup in Sec. II, in Sec. III we briefly discuss the symmetry properties of the nonlinear second order susceptibility tensor and its relation to the measured quantities. In Sec. IV we present our time-resolved MSHG data and describe them by a phenomenological two-temperature model assuming an explicit (linear) temperature dependence of the magnetic *as well as the nonmagnetic* tensor elements of the nonlinear susceptibility. In Sec. V we compare this description with those used in the literature and conclude in Sec. VI that the Kerr measurements do *not prove* any ultrafast demagnetization on the sub-ps time scale.

II. EXPERIMENT

For the measurements a commercial Ti:sapphire regenerative laser amplifier which generates 150 fs pulses at a center wavelength of 800 nm with a repetition rate of 5 kHz was used. The laser beam was split into a pump and a probe beam by a beam splitter. The fluence of the probe beam was about 6 mJ/cm² in all measurements. In a computer controlled delay line the probe pulse could be variably delayed with respect to the pump pulse. A $\lambda/2$ plate followed by a polarizer allowed the variation of the pump fluence up to

8.1 mJ/cm². The polarization of the probe beam was controlled by a $\lambda/2$ plate. Dichroic filters blocked any second harmonic (SH) light generated in the incident beam path of the probe beam. For a more stable and homogeneous illumination of the sample spot hit by the probe beam the spot diameter of the pump beam was larger (1.2 mm) than that of the probe beam (0.8 mm). Because we detect the SH light the effective SH spot diameter was only 0.4 mm due to the Gaussian shape of the light pulses. The angle of incidence was 45° for the probe beam and 33.5° for the pump beam. After reflection from the sample the pump beam was blocked. The SH light generated by the probe pulse was separated from the fundamental light by interference filters and a colored glass filter (Schott BG39, 5 mm thick) and detected by a photomultiplier using boxcar integration. Zero time delay was determined by the maximum of the cross correlation signal. The detection unit was rotated by 5.8° in the optical plane about the sample for this purpose.

The sample was a Ni(110) single crystal, tempered in H₂ atmosphere after polishing. All measurements were performed in air at room temperature. During the measurements a magnetic field was applied along one of the $\langle 111 \rangle$ easy axes in the surface plane to keep the (static) magnetization of the sample at saturation. The sample was mounted between the poles of the yoke of a small electro magnet. Both yoke and crystal could be rotated about the surface normal. Measurements with the optical plane parallel (longitudinal Kerr geometry) and perpendicular (transverse Kerr geometry) to the direction of the magnetic field were realized by rotation of the yoke together with the crystal by 90°. For measurements in the longitudinal geometry a polarizer was placed in the outgoing path of the probe beam.

III. SYMMETRY PROPERTIES OF THE NONLINEAR SUSCEPTIBILITY

In the electric dipole approximation the nonlinear polarization $\mathbf{P}(2\omega)$ can be written as

$$P_i(2\omega) = \chi_{ijk}^{(2)} E_j(\omega) E_k(\omega),$$

$\chi_{ijk}^{(2)}$ is the second-order optical susceptibility tensor and $\mathbf{E}(\omega)$ the electric field amplitude of the incident light. Due to the low symmetry of the system in our case all elements of $\chi_{ijk}^{(2)}$ contribute. However, the 180° rotation about the surface normal is equivalent to a magnetization reversal. The presence of such a symmetry operation allows us to classify the tensor elements as being even (nonmagnetic tensor element) or odd (magnetic tensor element) under magnetization reversal. For a fixed geometry all contributing tensor elements can be combined into one effective magnetic tensor element χ_m and one nonmagnetic tensor element χ_{nm} . While χ_{nm} is independent of M , χ_m is proportional to M in the first approximation.¹⁶ The observed magneto-optical effects are similar to those in the linear reflected light. For the magnetization in the optical plane a change in the polarization state is observed while for the magnetization perpendicular to the optical plane a change in the SH intensity upon magnetization reversal is observed. The measured SH intensities for opposite magnetization directions I_\uparrow and I_\downarrow , are given by

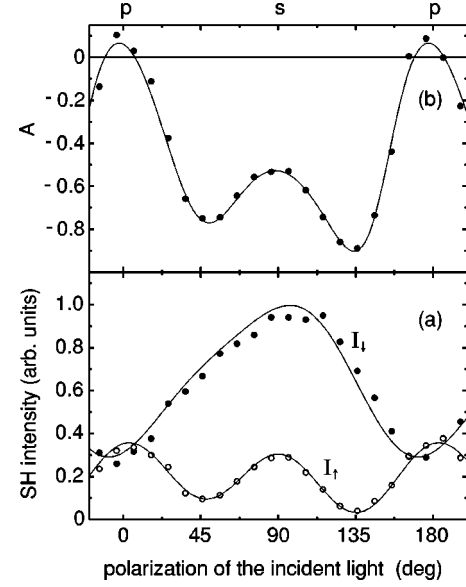


FIG. 1. (a) Second harmonic (SH) intensities for opposite magnetization directions and (b) SH asymmetry A vs polarization of the incident light measured in transverse geometry. The Ni(110) sample was magnetized to saturation along the $[1\bar{1}\bar{1}]$ easy axis perpendicular to the optical axis. The lines are fitted to the data using the theoretical expression from asymmetry analysis.

$I_{\uparrow\downarrow} = |\chi_{nm}^{(2)} \pm \chi_m^{(2)} e^{i\phi}|^2$. From I_\uparrow and I_\downarrow the average SH intensity I_{ave} and the SH asymmetry A are calculated:

$$I_{ave} = \frac{I_\uparrow + I_\downarrow}{2} \quad A = \frac{I_\uparrow - I_\downarrow}{I_\uparrow + I_\downarrow}. \quad (1)$$

In Fig. 1 I_{ave} and A are plotted as a function of the polarization of the incident light for the transverse Kerr geometry. Because of the low symmetry of the system the curves are not symmetric with respect to the s or p polarization. Note, that for p -polarized incident light the SH asymmetry has the opposite sign (+) compared to that for s -polarized incident light (-). Different tensor elements of $\chi_{ijk}^{(2)}$, which may differ in amplitude and phase contribute to the SH intensity for the two polarization directions of the incident light and lead to the observed difference in sign.

For not too large asymmetry $|A| \leq 0.3$ as it is the case for all data presented in this paper, the relation of I_{ave} and A to the effective tensor elements χ_{nm} and χ_m can be written approximately (with an error of less than 2%)

$$I_{ave} \propto (\chi_{nm})^2 \quad \text{and} \quad A \approx 2 \frac{|\chi_m|}{|\chi_{nm}|} \cos \phi \quad (2)$$

with ϕ the complex phase between χ_m and χ_{nm} . Thus, the time dependence of $I_{ave}(\Delta t)$ after the pump pulse reflects solely the temporal evolution of χ_{nm} , while $A(\Delta t)$ is governed by both, χ_m and χ_{nm} (see below). The time dependence of χ_{nm} in $A(\Delta t)$ cannot be neglected *a priori* but must be checked for each individual case.

IV. RESULTS

Our results of the pump-probe experiment in the transverse Kerr geometry for p -polarized incident light are shown

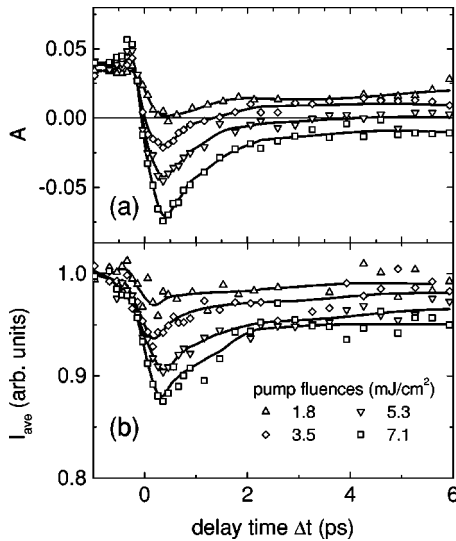


FIG. 2. (a) SH asymmetry A and (b) average SH intensity I_{ave} measured in transverse Kerr geometry with p -polarized incident light, as functions of the delay time Δt for various pump fluences (solid lines are guidelines to the eye).

in Fig. 2. The average intensity I_{ave} and the asymmetry A are plotted versus the delay time Δt for pump fluences between 1.8 and 7.1 mJ/cm^2 . The shapes of both curves $I_{\text{ave}}(\Delta t)$ and $A(\Delta t)$ are very similar for all pump fluences: a fast drop to a minimum at 300 fs and a relaxation within a few ps. $I_{\text{ave}}(\Delta t)$ and $A(\Delta t)$ scale linearly with the applied pump fluence. This is shown in Fig. 3 where I_{ave} and A are plotted against the fluence of the pump beam for a fixed delay time of 0.3 ps (open circles) and 3 ps (solid circles) after optical excitation. The observed linear dependence is in agreement with what was found by other authors.¹⁰

We observed a drop to $A=0$ already for a pump fluence of 1.8 mJ/cm^2 and a *negative* A for higher fluences. Obviously, the observed sign change at $\Delta t \leq 100$ fs cannot be attributed to a reversal of the magnetization caused by the

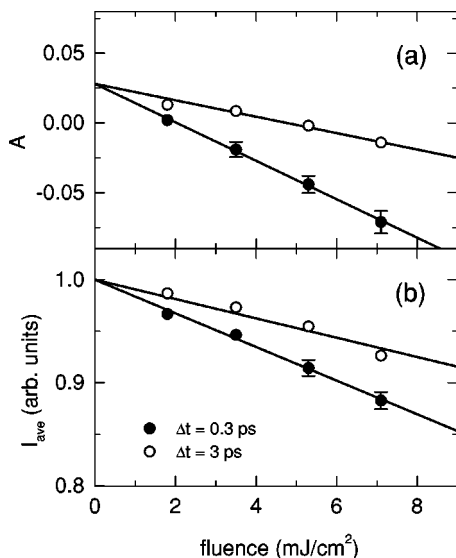


FIG. 3. (a) SH asymmetry A and (b) average SH intensity I_{ave} for a delay time Δt of 0.3 ps (solid circles) and 3 ps (open circles) after optical excitation as a function of the pump fluence.

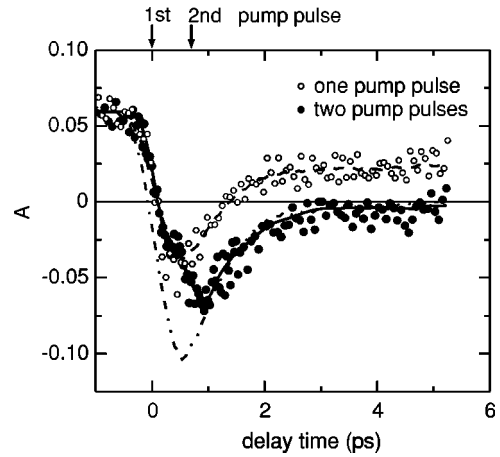


FIG. 4. SH asymmetry A vs delay time measured with one pump pulse at $\Delta t = 0$ ps (open circles, dashed line) and with two pump pulses at $\Delta t = 0$ ps and $\Delta t = 0.7$ ps (solid circles, solid line) with a pump fluences of 6.7 mJ/cm^2 for the first and 4.6 mJ/cm^2 for the second pump pulse (lines are guidelines to the eye). The dashed-dotted line represents the asymmetry curve expected for a single pump pulse at $\Delta t = 0$ with a fluence of 11.3 mJ/cm^2 , i.e., the sum of the fluences of the two pulses

magnetic field of the pump pulse. As it is already clear from not time-resolved measurements such sign changes of the nonlinear Kerr asymmetry as a function of an externally controlled parameter (other than the external magnetic field) such as thickness of a cover layer,^{17–19} temperature,²⁰ and adsorbate concentration^{21–23} may be simply the result of destructive interference of two SH sources or a phase change of the effective magnetic tensor element with respect to the nonmagnetic tensor element. Since the present experiments were carried out in air the Ni surface was covered by an oxide layer. Therefore it is very likely that SH is not only generated at the surface, but also at the oxide-layer–Ni interface. Since NiO is magnetically ordered an additional magnetic contribution from the surface to $\chi_{ijk}^{(2)}$ may arise. As NiO is transparent at $\lambda = 800$ nm, the oxide layer is not heated by the laser pulse. Heat diffusion from the hot Ni below is negligible on the time scale of a few ps because NiO is an insulator and therefore there is no heat transfer by conduction electrons. Thus, $I_{\text{ave}}(\Delta t)$ and $A(\Delta t)$ reflect the time dependence of $\chi_{ijk}^{(2)}$ of the oxide-layer–Ni interface only, while the magnetic and nonmagnetic contributions of the oxide layer contribute with a constant offset to the SH field amplitude. This is confirmed by the comparison of static and time resolved measurements shortly after polishing and tempering in H_2 atmosphere and after several days in air. For this experimental geometry the transverse geometry with p -polarized probe beam we observed a decrease in A after oxidation. The $A(\Delta t)$ curve was just shifted by a fixed amount towards lower values.

From the above it is already clear, that a reversal of A is not necessarily connected to a reversal of the magnetization. Furthermore, we can exclude not only this magnetization reversal but any coherent process by the following experiment: Two pump pulses separated by a fixed time delay of 0.7 ps precede the probe pulse and the SH intensity as a function of the delay time between these two pump pulses and the probe pulse was measured. The result is shown in Fig. 4. The flu-

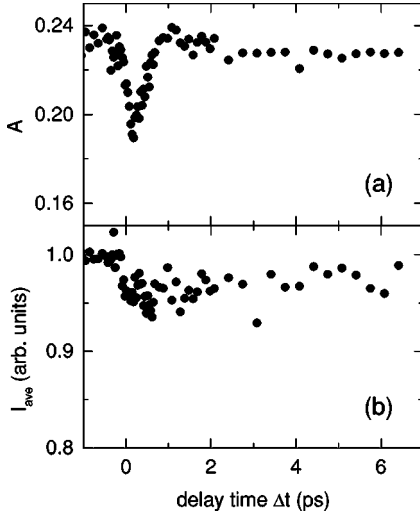


FIG. 5. (a) SH asymmetry A and (b) average SH intensity I_{ave} measured in longitudinal Kerr geometry with s -polarized probe beam. The polarizer in the beam of the outgoing SH light was set to 50° from p polarization. The fluence of the p -polarized pump beam was 8.1 mJ/cm^2 .

ence of the first pulse is 6.7 mJ/cm^2 and the fluence of the second pulse is 4.6 mJ/cm^2 . The combined effect of the two pump pulses is just the effect of a single pump pulse with a higher fluence of $(6.7+4.6) \text{ mJ/cm}^2$ for delay times after the second pump pulse (dash-dotted line in Fig. 4) indicating that there are no coherent processes left several 100 fs after the excitation. We did not observe a significant dependence of the SH intensity on the polarization state of the pump beam other than that caused by the difference in the absorption of the light.

Although for all investigated geometries and polarizations of the probe beam we found similar curves of the SH intensity vs delay time, the relative intensity changes after the pump pulse at 300 fs and at later times are different for each case. Figure 5 shows the transient MSHG signal measured in the longitudinal Kerr geometry with s -polarized incident light of the probe beam. The pump beam was p polarized as for the data shown in Fig. 2. Despite the high pump fluence of 8.1 mJ/cm^2 the change in I_{ave} as well as in A in the time evolution after the pump pulse is much weaker compared to the data in Fig. 2. Nevertheless, a sharp fast drop in A (and in I_{ave}) is still visible. However, opposite to the data presented in Fig. 2, A completely recovers after about 1 ps and there is only a very weak decrease at larger times. This result shows, that each tensor element of $\chi^{(2)}$ is differently affected by the pump pulse. The fact, that also the ratio of the change in I_{ave} and A for very short times of about 300 fs and at several ps differs, indicates the presence of two different relaxation processes.

In the following we compare our experimental results to the phenomenological two-temperature model initially proposed by Anisimov *et al.*^{24,25} The system is thought to consist of two subsystems, the electron system and the lattice having each its own temperature T_e and T_l , respectively. The two systems are assumed to be coupled weakly by the electron-phonon interaction term $g(T_e - T_l)$. The temporal development of the temperature profiles is described by the classical heat diffusion equation and the optical constants are

assumed to be a (linear) function of T_e . Also the magnetization is assumed to be a function of the electron temperature T_e alone.^{7,26}

We assume, that the time dependence of $\chi^{(2)}$ after the pump pulse can be described by the time dependence of the electron temperature alone. Then, to first approximation χ_{nm} depends linearly on T_e :

$$\chi_{\text{nm}}(T_e) = \chi_{\text{nm}}^0 + \chi_{\text{nm}}^1 T_e, \quad (3)$$

where χ_{nm}^0 is the effective nonmagnetic susceptibility at $T_e = 0 \text{ K}$ and χ_{nm}^1 the coefficient of the (linear) temperature dependence. Since $\chi_{\text{nm}}(T_e)$ is the effective susceptibility it also contains the change in the linear optical constants with temperature and depends on geometry and polarization. While χ_{nm} does not depend on the magnetization, χ_m does and therefore, an additional temperature dependence due to the temperature dependence of M has to be considered if the magnetization is affected by the pump pulse on the considered time scales.

$$\chi_m(T_e) = \chi_m^0 + \chi_m^1 M(T_e). \quad (4a)$$

For the temperature dependence of $M(T_e)$ we took the known (bulk) temperature dependence of the static magnetization.²⁷ In this case we neglect the intrinsic temperature dependence of χ_m against the much stronger one of M .

Equation (4a) is valid only if there is a strong change in the magnetization according to the bulk $M(T)$ dependence. If, however, the magnetization is not or only weakly affected on the ultrashort time scale, the intrinsic temperature dependence of $\chi_m(T_e)$ cannot be neglected. In this case a linear dependence

$$\chi_m(T_e) = \chi_m^0 + \chi_m^1 T_e \quad (4b)$$

is more appropriate.

For not too large $\chi_m(T_e)$ with respect to $\chi_{\text{nm}}(T_e)$ and the temperature coefficients χ_m^1 and χ_{nm}^1 small compared to χ_m^0 and χ_{nm}^0 , respectively, using Eq. (1) we find

$$I_{\text{ave}}(T_e) \approx I_{\text{ave}}^0 + I_{\text{ave}}^1 T_e \quad (5)$$

and

$$A(T_e) \approx A^0 \left(1 - \frac{I_{\text{ave}}^1}{I_{\text{ave}}^0} T_e \right) + A^1 M(T_e). \quad (6)$$

Since for all combinations of geometry and polarization of the probe beam we tested on the Ni(110) surface $\chi_{\text{nm}}^1 T_e / \chi_{\text{nm}}^0$ and $\chi_m^1 M(T_e) / \chi_m^0$ were of the same order of magnitude, the term $(-I_{\text{ave}}^1 T_e / I_{\text{ave}}^0)$ in Eq. (6) cannot be neglected and $A(T_e)$ is not governed by the temperature dependence of the magnetic tensor element alone.

To calculate the time dependence of the electron temperature T_e after the excitation with the pump pulse within the two-temperature model the values for the lattice heat capacity C_l , the electronic heat capacity $C_e = C_e' T_e$, the electronic heat conductivity κ_e , and the electron-lattice coupling constant g are needed. The values of these quantities given in the literature are usually determined in thermodynamic equilib-

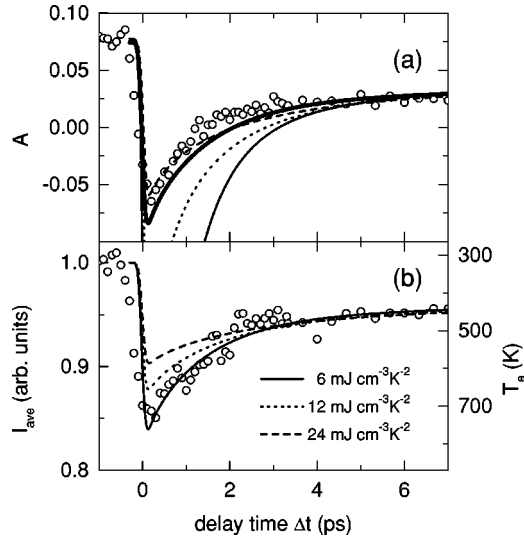


FIG. 6. (a) SH asymmetry A and (b) average SH intensity I_{ave} measured in transverse Kerr geometry with p -polarized incident light (open circles, left scales). The thin lines in (a) and (b) are theoretical lines according to Eqs. (3) and (4a), respectively, calculated within the two-temperature model for an electronic heat capacity of $C'_e = 6 \text{ mJ cm}^{-3} \text{ K}^{-2}$ (solid), $12 \text{ mJ cm}^{-3} \text{ K}^{-2}$ (dotted), and $24 \text{ mJ cm}^{-3} \text{ K}^{-2}$ (dashed line). For the solid curve ($C'_e = 6 \text{ mJ cm}^{-3} \text{ K}^{-2}$) the corresponding temperature scale T_e is plotted on the right side of (b). The thick solid line in (a) represents the calculation for $C'_e = 6 \text{ mJ cm}^{-3} \text{ K}^{-2}$ using a linear temperature dependence of χ_m according to Eq. (4b).

rium. These values may be changed after strong optical excitation. We found, that g can be varied over a relatively wide range (factor of 2) without affecting the $T_e(\Delta t)$ curve strongly. Similar is true for κ_e . However, C_e turned out to be a quite critical parameter because it essentially determines the maximum electron temperature reached after excitation.

The experimentally²⁷ and theoretically²⁸ determined value $C'_e = 1.1 \pm 0.2 \text{ mJ cm}^{-3} \text{ K}^{-2}$ for low temperatures may be significantly increased because of a large number of nonthermal electrons near the Fermi edge shortly after excitation, where the density of states of Ni shows strong peaks. Because no theoretical or experimental data quantifying this effect are currently available, we varied C'_e between the value given in Ref. 7, where $6 \text{ mJ cm}^{-3} \text{ K}^{-2}$ was used and $24 \text{ mJ cm}^{-3} \text{ K}^{-2}$. Furthermore we chose $g = 1 \times 10^{12} \text{ W/cm}^3 \text{ K}$, which is between the experimental⁷ and the theoretical value.²⁶ For the other parameter we have chosen $\kappa_e = 0.9 \text{ W/cm K}$ (Ref. 27), and $C_l = 3.8 \text{ mJ cm}^{-3} \text{ K}$.

Using Eqs. (5) and (6) $I_{\text{ave}}(\Delta t)$ and $A(\Delta t)$ were calculated from the $T_e(\Delta t)$ of the model. The parameters I_{ave}^0 and I_{ave}^1 and A^0 and A^1 were chosen in such a way, that the calculated curves agree with the measured curves at times before the pump pulse has reached the sample ($\Delta t = -2 \text{ ps}$) and at very long times ($\Delta t = 80 \text{ ps}$).

In Fig. 6 the result is shown for transverse Kerr geometry with p -polarized incident light. For $C'_e = 6 \text{ mJ cm}^{-3} \text{ K}^{-2}$ there is good agreement between the measured data of $I_{\text{ave}}(\Delta t)$ and the calculated $T_e(\Delta t)$. However, the asymmetry data points deviate strongly from the calculated $A(\Delta t)$ curve for $\Delta t \lesssim 3 \text{ ps}$. Using larger values for the electronic heat capacity improves the fit to A , while the fit to I_{ave} suffers.

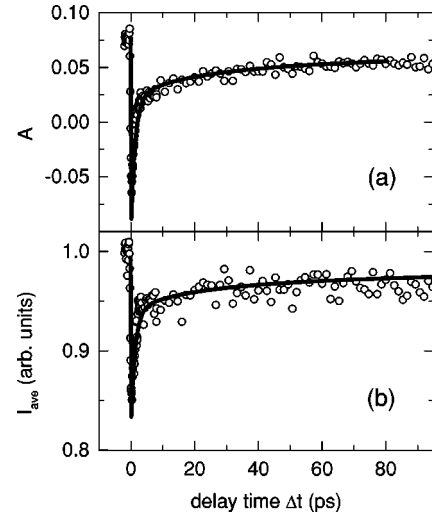


FIG. 7. (a) SH asymmetry A and (b) average SH intensity I_{ave} (solid circles) measured in transverse Kerr geometry with p -polarized incident light. The solid lines are the theoretical lines for $C'_e = 6 \text{ mJ cm}^{-3} \text{ K}^{-2}$ using a linear T_e dependence for I_{ave} as well as for A [Eqs. (3) and (4b)].

However, if we assume that the change of the magnetization is *negligible* and use a *linear* temperature dependence for χ_m as for χ_{nm} [Eqs. (3) and (4b)] the calculation agrees best with the measured data down to 300 fs as shown in Fig. 6(a) as thick line. This good fit can be achieved over the entire investigated range of delay times up to 80 ps as it is shown in Fig. 7.

V. DISCUSSION

As mentioned in the Sec. I other authors attributed the ultrafast change of the Kerr signal to a change of the magnetization induced by the high electron temperature. Hohlfeld *et al.* suggest in Ref. 10 that χ_{nm} was in first approximation independent of T_e and the temperature dependence of their average SH intensity $I^+ (= 2I_{\text{ave}}$ in our quantities) and their magnetic signal $I^- (= 2AI_{\text{ave}})$ was given solely by $\chi_m(T_e) = \gamma |M(T_e)|$. As the dependence of I^+ on M is only of second order their measured induced change in I^+ is too large to be consistent with the model. Calculations by Knorren and Bennemann²⁶ based on the data and the model proposed in Ref. 10 describe the temporal evolution of the average SH intensity and the Kerr signal only qualitatively. Partial agreement with the measured data is achieved *only* by setting $\chi_m/\chi_{\text{nm}} = 0.9$ and a phase ϕ close to 90° . However, Hohlfeld *et al.* derived from their measurements a value of $\chi_m/\chi_{\text{nm}} = 0.11$ and a phase $\phi = 0^\circ$.¹¹ There is obviously an inconsistency between model and experiment. Therefore, in Ref. 11 an alternative model was used assuming a linear temperature dependence of χ_{nm} , but still for χ_m only the temperature dependence due to a magnetization change was assumed as in Eq. (4a).

Our calculations show that no magnetization change has to be involved for a quantitative description of both $I_{\text{ave}}(\Delta t)$ and $A(\Delta t)$ with the phenomenological two-temperature model, if one permits individual temperature dependencies for different tensor elements, (i.e., considering a *direct* temperature dependence of χ_m as well). This is quite reasonable

as different $\chi_{ijk}^{(2)}$ involve transitions between different electronic states for each tensor element. An additional temperature dependence of χ_m describing a change of the thermodynamic magnetization M is not detectable in the given data, but of course cannot be excluded.

The two-temperature model seems to describe our data very well for delay times as short as 0.3 ps. However, this is not generally true as can be seen from the data in Fig. 5 for s -polarized incident light in the longitudinal Kerr geometry. A reasonably good fit is only possible for $\Delta t \geq 2$ ps. Obviously a thermodynamic description of the time dependencies for such short times is not possible. As the dephasing time of the coherent electronic state after optical excitation is only a few femtoseconds, the recovery cannot be explained in terms of such a dephasing. This is also corroborated by the result of the pump-probe experiment with two pump pulses shown in Fig. 4.

The origin of Kerr signal is the spin-orbit coupling in combination with the difference in the density of states of majority and minority spin electrons. As soon as the system is (strongly) optically excited the joint density of states is modified. Thus, an instantaneous change of I_\uparrow and I_\downarrow , and therefore of $I_{\text{ave}}(\Delta t)$ as well as of $A(\Delta t)$ may be observed. This change in A is not necessarily related to a change of the magnetization, since in the dipole approximation optical transitions between spin-up and spin-down states are not allowed. The temporal evolutions of χ_{nm} and χ_m or $I_{\text{ave}}(\Delta t)$ and $A(\Delta t)$, respectively, depend on the lifetimes of the involved electronic states. Aeschlimann *et al.*²⁹ found by spin resolved two photon photoemission that in ferromagnets the lifetime of excited minority spin electrons is larger than that of majority spin electrons. The lifetime of the electrons in transition metals is only about 20 fs for excitation energies of about 0.5 eV above E_F . However, for electrons close to E_F the lifetime increases up to the ps range for thermal excitation energies. In optical experiments discussed in this paper the whole deexcitation cascade contributes to the signal with a strong weight of the low excitation energies — not only the excited state initially populated by the pump pulse. Therefore, the observed strong dip at about 300 fs in the asymmetry curve in Fig. 5 could be caused by the different lifetime of minority and majority spin electrons because the initial imbalance of the lifetime prevails in the deexcitation cascade until full thermalization is achieved.

Time-resolved measurements of the Kerr ellipticity from ferromagnetic CoPt₃ films using left- and right-circular polarized pump light detected two distinct processes.⁹ One is a nonthermal, coherent process (depending on the polarization state of the pump beam) observable for delay times below ≈ 1 ps. This coherent process was explained as the decay of the photo induced spin polarization created in the excited states by the (circular polarized) pump pulse. We did not see a significant dependence on the pump beam polarization, in our experiments but this may be due to the in-plane magnetization and the use of linearly polarized pump light. For a perpendicularly magnetized ferromagnet, we would expect a similar dependence on the pump polarization. The authors of Ref. 9 observed also a thermal process which they assigned to a transient magnetization with a rise time of about 1.6 ps and a decay time of about 20 ps. The fact, that the linear Kerr effect cannot be thought of being proportional to the magne-

tization in the ultrashort time scale below 1 ps is also supported by the recent experiment of Koopmans *et al.*³⁰ They observed a different time dependence for the transient Kerr rotation and the Kerr ellipticity, clearly ruling out a simple linear dependence on the magnetization.

An experimental indication that demagnetization might occur on the time scale of a few ps is given in the recent time-resolved MSHG measurements on ultrathin Ni Films on Cu(001) by Gdde *et al.*^{31,12} Due to the reduced Curie temperature T_C in such thin films the electron temperature could be kept a longer time above T_C after the pump pulse leading to an almost constant (zero) asymmetry up to $\Delta t = 2$ ps, where T_e dropped below T_C and A started to increase again. This flat bottom in the $A(\Delta t)$ curve is not present in the average SH intensity curve $I_{\text{ave}}(\Delta t)$. Also the variation of the SH intensity and asymmetry in static measurements (without pump pulse) as a function of the sample temperature is in agreement with those observed in the transient signals.

Common spin-relaxation mechanisms such as spin-lattice relaxation fail to explain such a fast demagnetization processes. The spin-lattice relaxation time is given by the spin-orbit-induced magnetocrystalline anisotropy energy,³² which even for materials such as Gd or Au results in relaxation times of several ten ps.^{6,1} Hbner and Zhang showed that the magnetic as well as nonmagnetic elements of $\chi^{(2)}$ relax within a few 10 fs after optical excitation.¹³ The dephasing of the wave functions on this very short time scale alone is responsible for the changed MSHG signals. This model included no loss channel allowing a transfers of energy or angular momentum from the electronic system to the lattice. Thus, despite the observed change of χ_m the magnetization was not or (including spin-orbit interaction) only weakly affected. However, in their recent model calculations, taking explicitly the laser field into account, they showed that the combined action of laser field and spin-orbit coupling can lead to a strong reduction of the magnetization within the duration of the laser pulse.³³ Since the demagnetization occurs within the duration of the laser pulse it cannot be resolved in the experiments and appears as an instantaneous drop in A . However, whether such an instantaneous drop of the magnetization occurs or not is not yet confirmed experimentally.

VI. CONCLUSION

We have shown, that the transient Kerr signal in the SHG from a Ni(110) crystal surface can be described by a *linear* temperature dependence of the magnetic and nonmagnetic tensor elements of the second order susceptibility χ_m and χ_{nm} within the two-temperature model without invoking any additional temperature dependence of χ_m due to a (possibly) reduced magnetization. While there is some evidence that the magnetization can be reduced within a few ps, on the time scale below ≈ 2 ps a thermodynamic description fails and therefore a direct determination of the magnetization from Kerr measurements is not possible in the fs time scale.

ACKNOWLEDGMENT

The work was supported in part by the EC through Grant No. RB-EMRX-CT96-0015 (TMR NOMOKE).

- ¹A.Y. Elezzabi, M.R. Freeman, and M. Johnson, Phys. Rev. Lett. **77**, 3220 (1996).
- ²W.K. Hiebert, A. Stankiewicz, and M.R. Freeman, Phys. Rev. Lett. **79**, 1134 (1997).
- ³G. Ju, A.V. Nurmikko, R.F.C. Farrow, R.F. Marks, M.J. Carrey, and B.A. Gurney, Phys. Rev. Lett. **82**, 3705 (1999).
- ⁴T.M. Crawford, T.J. Silva, C.W. Teplin, and C.T. Rogers, Appl. Phys. Lett. **74**, 3386 (1999).
- ⁵C.H. Back, D. Weller, J. Heidmann, D. Mauri, D. Guarisco, E.L. Garwin, and H.C. Siegmann, Phys. Rev. Lett. **81**, 3251 (1998).
- ⁶A. Vaterlaus, T. Beutler, and F. Meier, Phys. Rev. Lett. **67**, 3314 (1991).
- ⁷E. Beaupaire, J.-C. Merle, A. Daunois, and J.-Y. Bigot, Phys. Rev. Lett. **76**, 4250 (1996).
- ⁸E. Beaupaire, M. Maret, V. Halte, J.-C. Daunois, and J.-Y. Bigot, Phys. Rev. B **58**, 12 134 (1998).
- ⁹G. Ju, A. Vertikov, A.V. Nurmikko, C. Canady, G. Xiao, R.F.C. Farrow, and A. Cebollada, Phys. Rev. B **57**, R700 (1998).
- ¹⁰J. Hohlfield, E. Matthias, R. Knorren, and K.H. Bennemann, Phys. Rev. Lett. **78**, 4861 (1997).
- ¹¹J. Hohlfield, J. Gddde, U. Conrad, O. Dhr, G. Korn, and E. Matthias, Appl. Phys. B: Lasers Opt. **68**, 505 (1999).
- ¹²U. Conrad, J. Gddde, V. Jhnke, and E. Matthias, Appl. Phys. B: Lasers Opt. **68**, 511 (1999).
- ¹³W. Hbner and G.P. Zhang, Phys. Rev. B **58**, R5920 (1998).
- ¹⁴G.P. Zhang and W. Hbner, J. Appl. Phys. **85**, 5657 (1999).
- ¹⁵A. Scholl, L. Baumgarten, R. Jacquemin, and W. Eberhardt, Phys. Rev. Lett. **79**, 5146 (1997).
- ¹⁶U. Pustogowa, W. Hbner, and K.-H. Bennemann, Surf. Sci. **307-309**, 1129 (1994).
- ¹⁷R. Vollmer, in *Nonlinear Optics at Metallic Interfaces*, edited by K.-H. Bennemann (Oxford University Press, Oxford, 1998), Chap. 2, p. 42–131.
- ¹⁸Q.Y. Jin, H. Regensburger, R. Vollmer, and J. Kirschner, Phys. Rev. Lett. **80**, 4056 (1998).
- ¹⁹R. Vollmer, Q.Y. Jin, H. Regensburger, and J. Kirschner, J. Magn. Magn. Mater. **198-199**, 611 (1999).
- ²⁰Q.Y. Jin, H. Regensburger, R. Vollmer, and J. Kirschner, Appl. Phys. Lett. **85**, 5288 (1999).
- ²¹K.J. Veenstra, P.E. Hansen, A. Kirilyuk, A.V. Petukhov, and T. Rasing, J. Magn. Magn. Mater. **198-199**, 695 (1999).
- ²²R. Vollmer, M. Straub, and J. Kirschner, J. Magn. Soc. Jpn. **20**, 29 (1996).
- ²³R. Vollmer, M. Straub, and J. Kirschner, Surf. Sci. **352**, 937 (1996).
- ²⁴S.I. Anisimov, B.L. Kapeliovich, and T.L. Perel'man, Zh. Éksp. Teor. Fiz. **66**, 776 (1974) [Sov. Phys. JETP **39**, 375 (1974)].
- ²⁵Rate equations describing heat diffusion (one dimension) in electrons (e) and lattice (l) in the two-temperature model: $C_e(\partial/\partial t)T_e = (\partial/\partial z)\kappa_e(\partial/\partial z)T_e - g(T_e - T_l) + A(t; z)$, $C_l(\partial/\partial t)T_l = g(T_e - T_l)$, with C_e , C_l the specific heat of electrons and lattice, κ the heat conductivity, g the electron-phonon coupling constant, and $A(t; z)$ a source term describing the laser pulse.
- ²⁶R. Knorren and K.H. Bennemann, Appl. Phys. B: Lasers Opt. **68**, 501 (1999).
- ²⁷M.B. Stearns, in *Magnetic Properties of 3d, 4d, and 5d Elements, Alloys and Compounds*, edited by H.P.J. Wijn, Landolt-Brnstein, New Series, Group III, Vol. 19, Pt. a (Springer-Verlag, Berlin, 1986).
- ²⁸M. Shimizu, Physica B **91**, 14 (1977).
- ²⁹M. Aeschlimann, M. Bauer, S. Pawlik, W. Weber, R. Burmeister, D. Oberli, and H.C. Siegmann, Phys. Rev. Lett. **79**, 5158 (1997).
- ³⁰B. Koopmans, M. van Kampen, J.T. Kohlhepp, and W.J.M. de Jonge, J. Appl. Phys. (to be published).
- ³¹J. Gddde, U. Conrad, V. Jhnke, J. Hohlfield, and E. Matthias, Phys. Rev. B **59**, R6608 (1999).
- ³²W. Hbner and K.H. Bennemann, Phys. Rev. B **53**, 3422 (1996).
- ³³G.P. Zhang and W. Hbner (unpublished).